HHS Public Access

Author manuscript

Int J Obes (Lond). Author manuscript; available in PMC 2021 May 19.

Published in final edited form as:

Int J Obes (Lond). 2021 January ; 45(1): 143–154. doi:10.1038/s41366-020-00712-2.

Identification of gut microbiota and microbial metabolites regulated by an anti-microbial peptide lipocalin 2 in high fat diet-induced obesity

Xiaoxue Qiu[1], **Marissa Macchietto**[2], **Xiaotong Liu**[3], **You Lu**[4], **Yiwei Ma**[1], **Hong Guo**[1], **Milena Saqui-Salces**[5], **David A Bernlohr**[6], **Chi Chen**[1], **Steven Shen**[2], **Xiaoli Chen**[1,*]

[1]Department of Food Science and Nutrition, University of Minnesota, Twin Cities, MN 55455, USA.

[2]Clinical Translational Science Institute, University of Minnesota, Twin Cities, MN 55455, USA.

[3]Department of Computer Science and Engineering, Graduate Program in Bioinformatics and Computational Biology, University of Minnesota, Twin Cities, MN 55455, USA.

[4]Department of Plant and Microbial Biology, Microbial and Plant Genomics Institute, University of Minnesota, Twin Cities, MN 55455, USA.

[5]Department of Animal Science, University of Minnesota, Twin Cities, MN 55455, USA.

[6]Department of Biochemistry, Molecular Biology and Biophysics, University of Minnesota, Twin Cities, MN 55455, USA.

Abstract

Lipocalin 2 (Lcn2), as an anti-microbial peptide is expressed in intestine, and the upregulation of intestinal Lcn2 has been linked to inflammatory bowel disease. However, the role of Lcn2 in shaping gut microbiota during diet-induced obesity (DIO) remains unknown. We found that short-term high fat diet (HFD) feeding strongly stimulates intestinal Lcn2 expression and secretion into the gut lumen. As the HFD feeding prolongs, fecal Lcn2 levels turn to decrease. Lcn2 deficiency accelerates the development of HFD-induced intestinal inflammation and microbiota dysbiosis. Moreover, Lcn2 deficiency leads to the remodeling of microbiota-derived metabolome, including decreased production of short-chain fatty acids (SCFAs) and SCFA-producing microbes. Most importantly, we have identified Lcn2-targeted bacteria and microbiota-derived metabolites that potentially play roles in DIO and metabolic dysregulation. Correlation analyses suggest that Lcn2-targeted Dubosiella and Angelakisella have a novel role in regulating SCFAs production and

[*]**Corresponding author:** Xiaoli Chen, PhD, Department of Food Science and Nutrition, University of Minnesota-Twin Cities, St. Paul, MN 55108-1038, xlchen@umn.edu.

Author contributions

X.Q. designed and performed the experiments; analyzed the data including 16S rRNA sequencing data; wrote this article. M.M. analyzed 16S rRNA sequencing data and wrote part of the Methods. X.L. analyzed 16S rRNA sequencing data. X.Q. and Y.L. performed statistical analysis. Y.M. and H.G. performed the experiments. M.S. performed IHC data analysis and interpretation. D.B.A. conceived and designed the experiments. C.C. conceived and designed the experiments. S.S. conceived and designed 16S rRNA sequencing data analysis. X.C. conceived and designed the experiments, analyzed the data, and wrote the article.

Conflict of Interests

There were no potential conflicts of interest relevant to this article.

obesity. Our results provide a novel mechanism involving Lcn2 as an anti-microbial host factor in the control of gut microbiota symbiosis during DIO.

Keywords

lipocalin 2; gut microbiota; inflammation; obesity

Introduction

Gut microbiota functions as a key organ in regulating host metabolism and inflammation by producing bacterial metabolites and microbial-associated molecular patterns such as lipopolysaccharide (LPS). Bacterial metabolites have both a beneficial and detrimental impact on host physiology. For example, short-chain fatty acids (SCFAs) derived from indigestible fibers generally have anti-obesity and anti-diabetic properties [1–3], whereas circulating levels of branched-chain amino acids known to be affected by gut microbiota are associated with insulin resistance [4].

Obesity has been associated with chronic low-grade inflammation in multiple tissues including the bowel [5, 6]. Colonization of germ-free mice with “obese microbiota” results in an increase in body fat, confirming the role of gut microbiota in the pathogenesis of obesity [7]. However, how host factors contribute to the development of gut microbiota dysbiosis in diet-induced obesity (DIO) is unclear.

Lipocalin 2 (Lcn2) has been implicated in innate immunity. Mice lacking Lcn2 have increased susceptibility to bacterial infection and sepsis [8, 9]. In addition, Lcn2 has been shown to play an important role in metabolic inflammation in obesity and metabolic diseases. Our previous studies have demonstrated that Lcn2 expression was dramatically increased in adipose tissue of diet-induced obese mice [10]. Lcn2 deficiency exacerbates high fat diet (HFD)-induced adipose tissue inflammation and insulin resistance, as well as impairs adaptive thermogenesis [11, 12]. We also reported that Lcn2 overexpression in adipose tissue is beneficial for the maintenance of metabolic health during aging [13].

Lcn2 can be produced by epithelial and myeloid cells in the gut [14]. At the molecular level, Lcn2 has a typical β-barrel structure that encircles a central binding grove [15]. This structure allows Lcn2 to be capable of binding small molecules including siderophores and to act as an anti-microbial peptide. Siderophores are required for bacteria to acquire iron for growth. Due to its capability to capture enterobactin-type siderophores, Lcn2 is able to suppress the growth of siderophore-dependent bacteria mainly pathogenic bacteria belonging to the phylum of Proteobacteria, such as *Escherichia coli* [16]. Increasing evidence indicates that Lcn2 is involved in the pathogenesis of inflammatory bowel disease (IBD) and intestinal inflammation [17, 18]. Lcn2 deficiency confers thrives of enterobactin-producing bacteria in the inflamed gut [19]. Moreover, a specific bacterial species *Alistipes* spp. has been identified to be increased in colitis developed in Lcn2 and IL-10 double knockout mice [20], suggesting a role of Lcn2 in shaping gut microbiota during inflammation. However, little is known about the role Lcn2 plays in obesity-associated

microbiota dysbiosis. In this study, we investigated the role of Lcn2 as an anti-microbial factor in the control of gut microbial structure in HFD-induced obesity.

We report for the first time that long-term HFD feeding disrupts the secretion of Lcn2 leading to decreased fecal Lcn2 levels. Lcn2 deficiency alters microbial structure and reprograms microbial metabolism. Additionally, we identify novel bacteria that are specifically regulated by Lcn2 and potentially contribute to the pathogenesis of obesity and metabolic dysregulation.

Materials and Methods

Animals.

C57BL/6J mice were purchased from Jackson Laboratory (Bar Harbor, ME). Wild-type (WT) and global Lcn2 knockout (LKO) mice were maintained on a C57BL/6J background by heterozygous breeding scheme, as previously described [8]. Animals were housed with a 12-h light-dark cycle in a specific pathogen-free facility at the University of Minnesota. Male mice were weaned at the age of 4 weeks, followed by a regular chow diet (RCD) for 4 weeks to allow them to shape RCD-fed gut microbiota. At the age of 8 weeks, male mice were fed with a HFD containing fat calories: 60% lard (https://www.bio-serv.com/product/HFPellets.html) (Bio-Serv F3282, New Brunswich, NJ) for 2, 4, 8, 12, and 16 weeks. Age-matched (± 1 week) male mice were separately housed by genotype (2–3 mice/cage). After mice were sacrificed, gut tissues including small intestine (duodenum: 5–7cm from stomach, jejunum: 15 cm following duodenum, ileum: 10cm from cecum), cecum, and colon were collected, cleaned and washed with PBS, and snap-frozen in liquid nitrogen, followed by −80°C storage until homogenization. All the animal studies were approved by IACUC of University of Minnesota. Animal handling followed the National Institutes of Health guidelines.

Lipopolysaccharide Injection in Mice.

RCD-fed male C57BL/6 mice at the age of 12 weeks received intraperitoneal injection of lipopolysaccharide (LPS) at the dose of 0.3 mg/kg. Mice were then sacrificed after 3 hour(s) of LPS treatment. Colon tissues were collected for Lcn2 immunohistochemistry.

Isolation of Bacterial DNA and 16S rRNA Sequencing.

Stool samples were freshly collected from individual mouse (directly from the anus), snap-frozen in liquid nitrogen, and stored at −80°C until use. Total fecal DNA was extracted using a DNA stool mini kit (QIAGEN). Bacterial 16S rRNA were amplified using primers (515F and 806R) for the V4 region. After quantification, the PCR products were sequenced using the paired-end 300 bp with Illumina MiSeq platform at the University of Minnesota Genomics Center. The detailed bioinformatics analyses of 16S rRNA Sequencing are described in Supplemental Materials.

Relative Quantitative RT-PCR.

Total RNA was extracted from tissues using TRIzol (Invitrogen). cDNA was synthesized using High Capacity cDNA RT kit (ThermoFisher Scientific), followed by quantitative PCR

using PowerUP™ SYBR™ Green Master Mix (ThermoFisher Scientific). The mRNA levels were determined by StepOne Real-Time PCR system (Applied Biosystem) using ΔΔCt method for calculating the results. TATA box binding protein 2 was used as the internal reference gene. Primer sequences were shown in Supplementary Table 1.

Western Blotting.

Gut tissues, including small intestine (duodedum, jejunum, ileum), cecum, and colon were homogenized and lysed using RIPA buffer (Sigma-Aldrich) supplemented with protease inhibitors. Protein concentrations were measured using the bicinchoninic acid method. Equal amounts of proteins were loaded and separated on 10% SDS-PAGE, transferred to a nitrocellulose membrane and immunoblotted with indicated antibodies. Blots were visualized by enhanced chemiluminescence (ThermoFisher Scientific). Antibodies used in this study were anti-Lcn2 (R&D System), anti-NFκB (Santa Cruz), anti-phospho-NFκB and anti-β-actin (Cell Signaling Technology).

Quantification of Fecal Lcn2 by ELISA.

Fecal samples were homogenized following a protocol previously described [18]. Briefly, frozen stool samples were reconstituted in 10 volumes [v(μl)/w(mg)] of PBS containing 0.1% Tween 20 and protease inhibitors. After 10 min centrifugation at 12,000 rpm under 4°C, the supernatants were collected for the measurement of Lcn2 levels using mouse NGAL ELISA kit (BioLegend).

Metabolomics Analysis of Fecal Contents.

Fecal samples were prepared and derivatized with 2-hydrazinoquinoline (HQ) for detecting fatty acids or with dansyl chloride (DC) for detecting amino acids prior to the LC-MS analysis as previously described [21]. The supernatants derived from either HQ or DC reaction were subjected to LC-MS analysis using an Acquity ultra-performance liquid chromatography (UPLC) system (Waters, Milford, MA, USA). MassLynx™ and SIMAC-P +™ software (Waters, Milford, MA, USA) were used for mass chromatograms and mass spectral data acquisition and procession.

Histology and Immunohistochemistry.

Gut tissues were fixed in 10% neutral buffered formalin overnight and then transferred into 70% ethanol. Paraffin embedding and hematoxylin & eosin staining were performed following a standard procedure. Immunohistochemistry (IHC) was carried out using VECTASTAIN Elite ABC-HRP Kit (ThermoFisher Scientific) and ImmPACT DAB Peroxidase substrate Kit (ThermoFisher Scientific) following the manufacturer's instruction. Antibodies used for IHC include Anti-CD11c (Cell Signaling Technology) and Anti-Lcn2 (ThermoFisher Scientific).

Statistical Analysis.

All results are shown as mean ± SEM. All data were assessed for homogeneity of variance by Levene's test or by boxplots for visual examination. The normality of data was assessed by Shapiro-Wilk test or by plotting with the qqnorm function in R environment (version

4.0.0). For normally distributed data with equal variance, the differences between groups were determined using one-way or two-way ANOVA followed by post-hoc Tukey's test, or two-tailed unpaired Student's t-test. Data were analyzed by repeated measures ANOVA when satisfying sphericity by Mauchly's test. Accordingly, non-normally distributed longitudinal data violating the assumption of homogeneity of variance were analyzed by a linear quantile mixed model (LQMM) modelling medians. The R package lqmm (version 1.5.5) was applied to perform LQMM using the lqmm function with the following settings: fixed=variable ~ Diet*Genotype, random=~1, group=subject, tau=0.5. *P*-values obtained from all the comparisons were adjusted to *q*-values using the qvalue package (version 2.16.0) via a false discovery rate (FDR)-based multiple testing correction procedure. The *q*-values less than 0.05 were considered as statistical significance. Data used for correlation analysis are non-normally distributed with unequal variance, and thus Spearman's correlation analysis was selected to evaluate the correlations. *P*-values of multiple comparison were corrected by the Benjamini-Hochberg method (Figure 6 and Supplementary Figure 7A). An adjusted *P*-value of less than 0.05 was considered statistically significant. All tests were two-tailed. Heatmaps were plotted using the pheatmap package (version 1.0.12) with row scaling. Hierarchical clustering using Euclidean distance and complete linkage was performed using the pheatmap function. All above statistics tests were performed using R (version 4.0.0).

Results

HFD feeding regulates Lcn2 expression in gut tissues and secretion into gut lumen.

We showed that Lcn2 protein levels were significantly increased in ileum, colon, and cecum of normal C57BL/6J male mice by 12 weeks of HFD feeding (Fig. 1A–D), whereas fecal Lcn2 levels were significantly decreased compared to RCD-fed mice (Fig. 1E). To determine the effect of a short-term HFD feeding on Lcn2 expression and secretion, mice were fed a HFD for 2 and 4 weeks, respectively. Interestingly, fecal Lcn2 levels were significantly elevated upon 2 weeks of HFD challenge, and then turn to decline after 4 weeks of HFD (Fig. 1F). Similarly, Lcn2 protein levels in colonic tissue were markedly increased in response to 2 weeks of HFD, but decreased after 4 weeks of HFD consumption (Supplementary Fig. 1A–1B). Additionally, the levels of phosphorylated NFkB were increased in the colon from mice fed a HFD for both 2 and 4 weeks (Supplementary Fig. 1A–1B), suggesting an inflammatory state in the gut tissues. Next, we performed immunohistology for the distribution of Lcn2 in the gut. Mice were treated for 3 hours with LPS, a potent stimulus of Lcn2 expression in multiple types of cells [10, 22–25]. We found that Lcn2 was dramatically induced by LPS in the gut, and Lcn2 positive staining was observed in colonic epithelial cells as well as innate immune cells (Supplementary Fig. 1C).

Lcn2 deficiency reduces gut microbial diversity during a short-term HFD feeding.

To examine the role of Lcn2 in shaping gut microbiota during DIO, we performed a time-course of HFD feeding on wild-type (WT) and Lcn2 knockout (LKO) mice. Microbial diversity, the richness (Chao1) reflecting the number of bacterial species, was significantly increased at 4 weeks of HFD in WT mice (Fig. 2A). However, this time-dependent change was not observed in LKO mice (Fig. 2A). Simpson which demonstrates both the richness

and evenness of bacteria was comparable between WT and LKO mice upon the HFD consumption. (Fig. 2A). Principal coordinate analysis (the Unweighted Unifrac) showed that the structure of gut microbial community was completely reshaped by the HFD feeding at all-time points, suggesting the effectiveness of dietary treatment (Fig. 2B). Importantly, an overall microbiota composition was different between WT and LKO mice when all time points were included for the analysis (Fig. 2B). Next, we explored the time-dependent effect of Lcn2 deficiency on HFD-induced reshaping of gut microbiota. As expected, the gut microbial community between WT and LKO mice was not significantly different prior to a HFD (Fig. 2C). The dissimilarity of gut microbial community between WT and LKO mice was observed at 2, 4, and 8 weeks of HFD feeding (Fig. 2C). Interestingly, after 16 weeks of HFD, the difference in gut microbiota composition disappeared (Fig. 2C). These findings suggest that Lcn2 has a protective role against the development of gut microbial dysbiosis during the early stage of DIO.

Lcn2 deficiency reshapes diet-induced gut microbiota composition in a time-dependent manner.

The taxonomic diversity analysis showed that the ratio of Firmicutes to Bacteroidetes (F/B) was increased in both WT and LKO mice upon the challenge of the short-term HFD feeding (Fig.3A and 3B). Strikingly, the F/B ratio was significantly higher in LKO mice than WT mice by 4 and 8 weeks of HFD (Fig. 3A and 3B). Moreover, the abundance of Actinobacteria, one of the four major phyla enriched in obese individuals [26–28] was significantly increased in LKO mice compared to WT controls upon 8 and 16 weeks of HFD (Fig. 3C). The abundance of Tenericutes, another phylum member was similar between WT and LKO mice during the entire period of HFD challenge (Fig. 3C).

At the bacterial family level (Fig. 3D), Erysipeotrichaceae which is higher in obesity [28], was increased by the HFD feeding in both WT and LKO mice, but not different between two genotypes (Fig. 3D). Muribaculaceae is positively correlated with the levels of short-chain fatty acids (SCFAs) - propionate [29], and its abundance was significantly decreased in both WT and LKO mice starting from 2 weeks of HFD feeding (Fig. 3D). Ruminococcaceae known to be associated with obesity and diabetes [30] was enriched in LKO mice compared to WT mice fed a HFD for 8 weeks (Fig.3D). Rikenellaceae has been reported as a protective bacterium in dextran sulfate sodium (DSS)-induced colitis [31]. Moreover, Rikenellaceae and its genus Rikenellaceae_RC9 are SCFA producers, which are beneficial for metabolic health. [32–34]. Interestingly, the abundances of Rikenellaceae and Rikenellaceae_RC9 were significantly lower in LKO mice compared to WT controls during the short-term HFD consumption (Fig. 3D and Supplementary Fig. 2A). Taken together, these data suggest that Lcn2 deficiency-associated gut microbiota dysbiosis is dependent on HFD treatment.

Next, a generalized linear model with host genotypes as fixed effect [35] was used to identify Lcn2-targeted bacteria at the genus level. While the abundances of 21 bacteria were significantly increased (Fig. 4A), 24 bacteria were significantly decreased (Fig. 4B) in LKO mice. Specifically, Dorea, Cuneatibacter, and Acetanaerobacterium thrived in LKO mice at 2 weeks of HFD challenge (Fig. 4A). The abundances of Angelakisella, Harryflintia, and

Intestinimonas were significantly increased in LKO mice during the entire period of HFD consumption (Fig. 4A and Supplementary Fig. 2A). Notably, Dubosiella which belongs to the family Erysipelotrichaceae, thrived in LKO mice under both the RCD and 2-week HFD-fed conditions (Fig. 4A and Supplementary Fig. 2B), indicating that the growth of Dubosiella is regulated by both gene and diet. More strikingly, the abundances of several SCFA-producing bacteria including Butyriccoccus, ASF (altered Schaedler flora) 356, Ruminococcus_1 and Lachnospiraceae were decreased in LKO mice during the HFD feeding (Fig. 4B). Interestingly, a group of bacteria including Romboutsia, Shuttleworthia, XBB1006, Candidatus Stoquelichus, Streptococcus, Anaerovorax, and Candidatus Soleaferrea thrived only in WT but not LKO mice upon the HFD challenge (Fig. 4B).

Lastly, the generalized linear model on amplicon sequence variants (ASV) analysis showed that WT and LKO mice had similar ASV distribution pattern under the RCD-fed condition (Supplementary Fig. 3). A completely different ASV distribution pattern between WT and LKO mice was observed after a dietary switch from RCD to HFD (Supplementary Fig 3). We identified 121 ASVs increased while 66 decreased in LKO mice compared to WT mice (Supplementary Fig. 3). A functional analysis on 16S rRNA sequencing by searching against the Piphillin and KEGG pathway database indicate that Lcn2 deficiency alters microbial functions in lipid (Supplementary Fig. 4A and 4B) and amino acid (Supplementary Fig. 4C) metabolism.

Lcn2 deficiency alters HFD-induced remodeling of microbial metabolites.

Using the LC-MS-based metabolomics analysis, we profiled fecal metabolites. The PCA model showed that WT and LKO mice had a similar profile of fecal metabolites under the RCD-fed condition (Fig. 5A). As expected, HFD feeding caused shifts of fecal metabolites in both WT and LKO mice when compared with RCD (Fig. 5A). Intriguingly, HFD feeding induced a clear time-dependent shift of fecal metabolites in WT mice, whereas this time-dependent effect of HFD was completely diminished in LKO mice. Specifically, 4 weeks of HFD was sufficient to shift fecal metabolites to a similar extent to that induced by 16 weeks in LKO mice (Fig. 5A). Therefore, a significant difference in the overall profile of fecal metabolites between WT and LKO mice occurred upon 4 weeks but not 16 weeks of HFD feeding (Fig. 5A). This suggests that Lcn2 deficiency accelerates the detrimental effect of HFD on reshaping of gut microbiota.

SCFAs including acetic acid, propionic acid and butyric acid, the main end products of colonic fermentation have been implicated in energy metabolism. The LC-MS analysis showed that all three SCFAs were significantly decreased in both WT and LKO mice upon 4 and 16 weeks of HFD challenge (Fig. 5B). Strikingly, the SCFAs levels were more profoundly decreased in LKO mice compared to WT mice primarily upon 4 weeks of HFD feeding (Fig. 5B). Additionally, the fecal concentrations of medium-chain fatty acids (caproic acid, caprylic acid, capric acid, and lauric acid) and two long-chain fatty acids (palmitic acid and oleic acid) were significantly higher, whereas myristic acid and palmitoleic acids were significantly lower in LKO mice compared to WT mice upon 4 weeks of HFD feeding (Supplementary Fig. 5).

The assessments of fecal amino acids revealed that the concentrations of glutamic acid, aspartic acid and lysine were significantly increased in LKO mice versus WT mice only after 16 weeks of HFD feeding (Fig. 5C). Additionally, the levels of branched-chain amino acids, citrulline, Threonine, ornithine and tryptophine (Supplementary Fig. 6) had a trend towards an increase in LKO mice 16 weeks after HFD feeding.

Identification of specific gut bacteria that potentially contribute to obesity-related metabolic phenotype in LKO mice.

In consistent with our previous study [11], LKO mice showed an increase in body weight (Supplementary Fig. 7A). We performed Spearman's correlation analyses of body weight with either fecal metabolites or genus bacteria to identify the bacteria and metabolites with strong associations with body weight. Of all fecal metabolites measured, 14 showed significant correlations with body weight, including 6 amino acids (positive correlation), 3 SCFAs (negative correlation), 3 MCFAs and 2 LCFAs (positive correlation) (Fig. 6). Of all bacteria, 18 bacteria had significant positive association and 18 negative association with body weight. We then conducted second Spearman's correlation analyses between the above-identified 14 fecal metabolites and 36 genus bacteria that have strong correlations with body weight. More interestingly, among those 14 identified metabolites, the abundances of SCFAs were significantly decreased (Fig. 5B), while the metabolites MCFAs, palmitic acid and aspartic acid were significantly increased in HFD-fed LKO mice compared to WT mice (Supplemental Fig. 5 and Fig. 5C). Additionally, of those 36 genus bacteria, four had either significantly increased abundance (Dubosiella and Angelakisella) or decreased abundance (Ruminococcus_1 and Caproiciproducens) in HFD-fed LKO mice (Fig. 4 and Fig. 6), suggesting a specific role of these 4 bacteria in the obesity-related metabolic phenotype in LKO mice through regulating microbial metabolites (Supplemental Fig. 7B)

Lcn2 deficiency promotes intestinal inflammation during a short-term HFD feeding.

The time-course of HFD-induced intestinal inflammation showed that the mRNA expression of inflammatory marker IFNγ was significantly upregulated in the colon of LKO mice compared to that of WT mice at 2 and 4 weeks of HFD challenge (Supplemental Fig. 8E), which is supported by increased colonic levels of phosphorylated NFκB in LKO mice upon 2 weeks (Fig. 7A–7B) but not 16 weeks of HFD feeding (Supplementary Fig. 8A–D). There was no significant difference in the mRNA expression levels of *IL-6*, *IL-1β*, *IL-17* and anti-inflammatory cytokines (IL-10 and Arg1), as well as genes involved in the regulation of gut barrier function between WT and LKO mice (Supplementary Fig. 8E–8G). Although the overall intestinal architecture was comparable between WT and LKO mice (Fig. 7C), the colon from LKO mice harbored more $CD11c^+$ cells than that from WT mice after 2 weeks of HFD (Fig. 7D–7E). Our data suggests that Lcn2 deficiency alters intestinal inflammation only during a short-term (2-week) HFD. As the progression of HFD feeding, the impact of Lcn2 deficiency on intestinal inflammation became less evident (Supplementary Fig. 8). However, the effect of Lcn2 deficiency on microbiota composition, dysbiosis, and microbial metabolites persists during all time points of HFD feeding. Taken together, our results suggest that Lcn2 regulates gut microbiota composition possibly through a direct mechanism of controlling the growth of certain bacteria during the development of DIO.

Discussion

Lcn2 has been shown to play a protective role against intestinal inflammation and microbiota dysbiosis in an IL-10 KO mouse model of colitis [20]. However, little is known about the role of Lcn2 in gut microbiota during diet-induced obesity. We found that Lcn2 production in the gut is strongly induced during the early stage of HFD-induced obesity. While Lcn2 expression levels in the gut tissues consistently increase, fecal Lcn2 concentrations reduce substantially with the prolonged HFD consumption. It is possible that the long-term HFD consumption impairs the secretion of Lcn2 into the gut lumen and disrupts the protective effect of Lcn2 on the intestinal homeostasis of microbiota and inflammation.

The evidence of increased cytokine expression, NFκB activation, and infiltration of innate immune cells in the colon of LKO mice after 2 weeks of HFD suggests that the early induction of intestinal Lcn2 by HFD has a protective role against the development of HFD-induced inflammation. Moreover, Lcn2 deficiency alters the effect of short-term HFD on gut microbiota composition, specifically the increased abundances of Dubosiella belonging to family Erysipelotrichaceae [36], Angelakisella belonging to family Ruminococcaceae [37], and Dorea linked with gut inflammation [38]. Interestingly, decreased gut microbial diversity and increased F/B ratio in LKO mice are observed primarily at 4 and 8 weeks of HFD consumption when fecal Lcn2 levels began to decline. This suggests that the temporary increase in fecal Lcn2 levels at 2 weeks of HFD is beneficial for preventing the development of gut microbiota dysbiosis.

Gut microbiota composition is reshaped in obese individuals [7, 26, 27, 39], which is characterized by dysbiosis, a decrease in microbiota diversity. In our time-course studies of HFD feeding, there was a dynamic change in gut microbiota. For example, the microbial diversity undergoes an increase at the early stage of DIO, followed by a slight decline. This phenomenon correlates with the dynamic alterations in fecal Lcn2 concentrations in WT mice. Interestingly, this time-dependent change of gut microbiota disappeared in LKO mice, supporting a protective role of Lcn2 against HFD-induced microbial dysbiosis. The dissimilarity of gut microbial structure between WT and LKO mice becomes small after 16 weeks of HFD challenge, which could be associated with the disappearance of the difference in the fecal Lcn2 levels between the two genotypes. Nevertheless, the difference in specific compositional features of bacteria remains. For example, LKO mice display increased phylum Actinobacteria and genre Angelakisella. Increased Actinobacteria has been related to gut bacterial changes in obesity [27, 40].

Similar to the disappearance of the dissimilarity in gut microbiota composition between WT and LKO mice, the difference in microbiota-derived metabolites disappears after 16 weeks of HFD. Indeed, the food intake is comparable between WT and LKO as described in our previous publication [11], and thus the changes in fecal metabolites could be largely explained by gut microbial alterations, instead of food intake. LKO mice have significantly lower levels of fecal SCFAs than WT mice after a short-term HFD feeding, which could be explained by a reduction in SCFA-producing bacteria such as Rikenellaceae [33] and Ruminococcus_1 [41]. Our Spearman’s correlation analyses indicate that the fecal levels of

all three SCFAs are negatively associated with body weight, supporting the conclusion that decreased abundance of SCFA-producing bacteria potentially contributes in part to the metabolic phenotype of LKO mice. Additionally, there is a significant difference between WT and LKO mice in the fecal levels of glutamic acid, aspartic acids and lysine after a long-term HFD feeding. Since the fecal amino acid pool is determined by multiple factors including diets, gut bacteria metabolism, turnover of colonic cells and intestinal absorption, the pathological functions of increased amino acids in LKO mice need to be further understood.

Lcn2 plays a role in controlling the growth of siderophore-dependent bacteria by sequestering iron availability in a systemic bacterial infection scenario [8]. However, it is unclear how Lcn2 regulates the growth of specific gut microbes. Previous studies have demonstrated that Lcn2 specifically controls the expansion of *Alistipes* spp in *IL10*$^{-/-}$ colitis mouse model [20]. In HFD-induced obesity, the abundance of Alistipes is not altered in LKO mice. Further, Dubosiella that has been recently identified as a novel member of the family Erysipeotrichaceae [28, 36] thrives particularly in the gut of HFD-fed obese LKO mice. From our correlation analyses, the expansion of Dubosiella and Angelakisella has a positive correlation with body weight but a negative correlation with fecal SCFAs, suggesting that these bacteria have a novel role in obesity-related microbial dysbiosis. Moreover, Lcn2 deficiency inhibits the growth of SCFA-producing bacteria such as Rikenellaceae [33] and Ruminococcus_1 [41]. All of the above-mentioned changes in gut microbiota could be linked to the decreased levels of fecal SCFAs in LKO mice and explain part of the mechanisms for the metabolic phenotype of LKO mice.

We found that Lcn2 deficiency exacerbates HFD-induced microbiota dysbiosis and alterations in microbial metabolites after 4 and 16 weeks of HFD without significantly worsening intestinal inflammation. For instance, the exacerbated intestinal inflammation, as evidenced by the increased number of CD11c^{+} cells, occurs in LKO mice upon 2 but not 4 weeks of HFD feeding, whereas the Dubosiella expansion was observed in LKO mice at 4 weeks of HFD. More interestingly, the genotypic difference in the abundance of specific gut microbes persists until 16 weeks of HFD feeding. These findings suggest that intestinal inflammation occurs in parallel with microbiota dysbiosis in LKO mice, and Lcn2 controls microbiota symbiosis through a direct mechanism.

In summary, we have identified Lcn2-targeted bacteria and microbial metabolites that may play roles in DIO and metabolic dysfunction. Our data indicate that during the early stage of DIO, the host defends against HFD-induced microbial dysbiosis by increasing Lcn2 levels in the gut lumen to maintain gut microbiota symbiosis (Supplemental Fig. 9). Loss of Lcn2 accelerates and exacerbates the development of HFD-induced microbial dysbiosis by thriving Dubosiella and Angelakisella, suppressing the growth of SCFA-producing bacteria, as well as altering other 41 Lcn2-targted bacteria (Supplemental Fig. 9). However, the long-term HFD consumption disrupts the defensive mechanism of Lcn2 by reducing Lcn2 levels in the gut lumen (Supplemental Fig. 9). Due to the loss of this Lcn2 defensive system, microbiota dysbiosis develops, thereby accelerating the development of obesity and metabolic dysregulation.

Supplementary Material

Refer to Web version on PubMed Central for supplementary material.

Acknowledgements

This work was supported by Allen Foundation Grant awarded to X.C., the General Mills Foundation Chair in Genomics for Healthful Foods to X.C., NIDDK Grant (R01 DK123042) awarded to X.C., and the Doctoral Dissertation Fellowship from the University of Minnesota to X.Q.

References

1. Lin HV, Frassetto A, Kowalik EJ Jr., Nawrocki AR, Lu MM, Kosinski JR, et al. Butyrate and propionate protect against diet-induced obesity and regulate gut hormones via free fatty acid receptor 3-independent mechanisms. PloS one. 2012;7(4):e35240.
2. Kimura I, Ozawa K, Inoue D, Imamura T, Kimura K, Maeda T, et al. The gut microbiota suppresses insulin-mediated fat accumulation via the short-chain fatty acid receptor GPR43. Nature communications. 2013;4:1829.
3. Chang PV, Hao L, Offermanns S, Medzhitov R. The microbial metabolite butyrate regulates intestinal macrophage function via histone deacetylase inhibition. Proceedings of the National Academy of Sciences of the United States of America. 2014;111(6):2247–52. [PubMed: 24390544]
4. Pedersen HK, Gudmundsdottir V, Nielsen HB, Hyotylainen T, Nielsen T, Jensen BA, et al. Human gut microbes impact host serum metabolome and insulin sensitivity. Nature. 2016;535(7612):376–81. [PubMed: 27409811]
5. Garidou L, Pomie C, Klopp P, Waget A, Charpentier J, Aloulou M, et al. The Gut Microbiota Regulates Intestinal CD4 T Cells Expressing RORgammat and Controls Metabolic Disease. Cell metabolism. 2015;22(1):100–12. [PubMed: 26154056]
6. Luck H, Tsai S, Chung J, Clemente-Casares X, Ghazarian M, Revelo XS, et al. Regulation of obesity-related insulin resistance with gut anti-inflammatory agents. Cell metabolism. 2015;21(4):527–42. [PubMed: 25863246]
7. Turnbaugh PJ, Ley RE, Mahowald MA, Magrini V, Mardis ER, Gordon JI. An obesity-associated gut microbiome with increased capacity for energy harvest. Nature. 2006;444(7122):1027–31. [PubMed: 17183312]
8. Flo TH, Smith KD, Sato S, Rodriguez DJ, Holmes MA, Strong RK, et al. Lipocalin 2 mediates an innate immune response to bacterial infection by sequestrating iron. Nature. 2004;432(7019):917–21. [PubMed: 15531878]
9. Berger T, Togawa A, Duncan GS, Elia AJ, You-Ten A, Wakeham A, et al. Lipocalin 2-deficient mice exhibit increased sensitivity to Escherichia coli infection but not to ischemia-reperfusion injury. Proceedings of the National Academy of Sciences of the United States of America. 2006;103(6):1834–9. [PubMed: 16446425]
10. Zhang J, Wu Y, Zhang Y, Leroith D, Bernlohr DA, Chen X. The role of lipocalin 2 in the regulation of inflammation in adipocytes and macrophages. Mol Endocrinol. 2008;22(6):1416–26. [PubMed: 18292240]
11. Guo H, Jin D, Zhang Y, Wright W, Bazuine M, Brockman DA, et al. Lipocalin-2 deficiency impairs thermogenesis and potentiates diet-induced insulin resistance in mice. Diabetes. 2010;59(6):1376–85. [PubMed: 20332347]
12. Jin D, Guo H, Bu SY, Zhang Y, Hannaford J, Mashek DG, et al. Lipocalin 2 is a selective modulator of peroxisome proliferator-activated receptor-gamma activation and function in lipid homeostasis and energy expenditure. FASEB journal : official publication of the Federation of American Societies for Experimental Biology. 2011;25(2):754–64. [PubMed: 20974668]
13. Deis JA, Guo H, Wu Y, Liu C, Bernlohr DA, Chen X. Adipose Lipocalin 2 overexpression protects against age-related decline in thermogenic function of adipose tissue and metabolic deterioration. Mol Metab. 2019;24:18–29. [PubMed: 30928474]

14. Devireddy LR, Gazin C, Zhu X, Green MR. A cell-surface receptor for lipocalin 24p3 selectively mediates apoptosis and iron uptake. Cell. 2005;123(7):1293–305. [PubMed: 16377569]
15. Xiao X, Yeoh BS, Vijay-Kumar M. Lipocalin 2: An Emerging Player in Iron Homeostasis and Inflammation. Annual review of nutrition. 2017;37:103–30.
16. Wilson BR, Bogdan AR, Miyazawa M, Hashimoto K, Tsuji Y. Siderophores in Iron Metabolism: From Mechanism to Therapy Potential. Trends Mol Med. 2016;22(12):1077–90. [PubMed: 27825668]
17. Stallhofer J, Friedrich M, Konrad-Zerna A, Wetzke M, Lohse P, Glas J, et al. Lipocalin-2 Is a Disease Activity Marker in Inflammatory Bowel Disease Regulated by IL-17A, IL-22, and TNF-alpha and Modulated by IL23R Genotype Status. Inflamm Bowel Dis. 2015;21(10):2327–40. [PubMed: 26263469]
18. Chassaing B, Srinivasan G, Delgado MA, Young AN, Gewirtz AT, Vijay-Kumar M. Fecal lipocalin 2, a sensitive and broadly dynamic non-invasive biomarker for intestinal inflammation. PloS one. 2012;7(9):e44328.
19. Raffatellu M, George MD, Akiyama Y, Hornsby MJ, Nuccio SP, Paixao TA, et al. Lipocalin-2 resistance confers an advantage to Salmonella enterica serotype Typhimurium for growth and survival in the inflamed intestine. Cell host & microbe. 2009;5(5):476–86. [PubMed: 19454351]
20. Moschen AR, Gerner RR, Wang J, Klepsch V, Adolph TE, Reider SJ, et al. Lipocalin 2 Protects from Inflammation and Tumorigenesis Associated with Gut Microbiota Alterations. Cell host & microbe. 2016;19(4):455–69. [PubMed: 27078067]
21. Lu Y, Yao D, Chen C. 2-Hydrazinoquinoline as a Derivatization Agent for LC-MS-Based Metabolomic Investigation of Diabetic Ketoacidosis. Metabolites. 2013;3(4):993–1010. [PubMed: 24958262]
22. Sunil VR, Patel KJ, Nilsen-Hamilton M, Heck DE, Laskin JD, Laskin DL. Acute endotoxemia is associated with upregulation of lipocalin 24p3/Lcn2 in lung and liver. Exp Mol Pathol. 2007;83(2):177–87. [PubMed: 17490638]
23. Glaros T, Fu Y, Xing J, Li L. Molecular mechanism underlying persistent induction of LCN2 by lipopolysaccharide in kidney fibroblasts. PloS one. 2012;7(4):e34633.
24. Borkham-Kamphorst E, van de Leur E, Zimmermann HW, Karlmark KR, Tihaa L, Haas U, et al. Protective effects of lipocalin-2 (LCN2) in acute liver injury suggest a novel function in liver homeostasis. Biochimica et biophysica acta. 2013;1832(5):660–73. [PubMed: 23376114]
25. Kang SS, Ren Y, Liu CC, Kurti A, Baker KE, Bu G, et al. Lipocalin-2 protects the brain during inflammatory conditions. Molecular psychiatry. 2018;23(2):344–50. [PubMed: 28070126]
26. Hildebrandt MA, Hoffmann C, Sherrill-Mix SA, Keilbaugh SA, Hamady M, Chen YY, et al. High-fat diet determines the composition of the murine gut microbiome independently of obesity. Gastroenterology. 2009;137(5):1716–24 e1–2. [PubMed: 19706296]
27. Turnbaugh PJ, Hamady M, Yatsunenko T, Cantarel BL, Duncan A, Ley RE, et al. A core gut microbiome in obese and lean twins. Nature. 2009;457(7228):480–4. [PubMed: 19043404]
28. Zhang H, DiBaise JK, Zuccolo A, Kudrna D, Braidotti M, Yu Y, et al. Human gut microbiota in obesity and after gastric bypass. Proceedings of the National Academy of Sciences of the United States of America. 2009;106(7):2365–70. [PubMed: 19164560]
29. Smith BJ, Miller RA, Ericsson AC, Harrison DE, Strong R, Schmidt TM. Changes in the gut microbiota and fermentation products associated with enhanced longevity in acarbose-treated mice. BMC Microbiology. 2019;19:130. [PubMed: 31195972]
30. Kim K-A, Gu W, Lee I-A, Joh E-H, Kim D-H. High fat diet-induced gut microbiota exacerbates inflammation and obesity in mice via the TLR4 signaling pathway. PloS one. 2012;7(10):e47713.
31. Macia L, Tan J, Vieira AT, Leach K, Stanley D, Luong S, et al. Metabolite-sensing receptors GPR43 and GPR109A facilitate dietary fibre-induced gut homeostasis through regulation of the inflammasome. Nat Commun. (2015);6:6734. [PubMed: 25828455]
32. Zhernakova A, Kurilshikov A, Bonder MJ, Tigchelaar EF, Schirmer M, Vatanen T, et al. Population-based metagenomics analysis reveals markers for gut microbiome composiiton and diversity. Science. 2016; 352:565–9. [PubMed: 27126040]
33. Louis P, Flint HJ. Formation of porpionate and butyrate by the human colonic microbiota. Environmental Microbiology. 2017; 19(1):29–41. [PubMed: 27928878]

34. Holman DB, Gzyl KE. A meta-analysis of the bovine gastrointestinal tract microbiota. FEMS Microbiology Ecology. 2019; 95(6):fiz072.

35. Hillmer RA, Tsuda K, Rallapalli G, Asai S, Truman W, Papke MD, et al. The highly buffered Arabidopsis immune signaling network conceals the functions of its components. PLoS genetics. 2017;13(5):e1006639.

36. Cox LM, Sohn J, Tyrrell KL, Citron DM, Lawson PA, Patel NB, et al. Description of two novel members of the family Erysipelotrichaceae: Ileibacterium valens gen. nov., sp. nov. and Dubosiella newyorkensis, gen. nov., sp. nov., from the murine intestine, and emendation to the description of Faecalibaculum rodentium. Int J Syst Evol Microbiol. 2017;67(5):1247–54. [PubMed: 28100298]

37. Mailhe M, Ricaboni D, Vitton V, Cadoret F, Fournier PE, Raoult D. 'Angelakisella massiliensis' gen. nov., sp. nov., a new bacterial species isolated from human ileum. New Microbes New Infect. 2017;16:51–3. [PubMed: 28203377]

38. Shahi SK, Freedman SN, Mangalam AK. Gut microbiome in multiple sclerosis: The players involved and the roles they play. Gut Microbes. 2017;8(6):607–15. [PubMed: 28696139]

39. Ley RE, Backhed F, Turnbaugh P, Lozupone CA, Knight RD, Gordon JI. Obesity alters gut microbial ecology. Proceedings of the National Academy of Sciences of the United States of America. 2005;102(31):11070–5. [PubMed: 16033867]

40. Everard A, Lazarevic V, Gaia N, Johansson M, Stahlman M, Backhed F, et al. Microbiome of prebiotic-treated mice reveals novel targets involved in host response during obesity. ISME J. 2014;8(10):2116–30. [PubMed: 24694712]

41. Mao Z, Ren Y, Zhang Q, Dong S, Han K, Feng G, et al. Glycated fish protein supplementation modulated gut microbiota composition and reduced inflammation but increased accumulation of advanced glycation end products in high-fat diet fed rats. Food Funct. 2019;10(6):3439–51. [PubMed: 31139782]

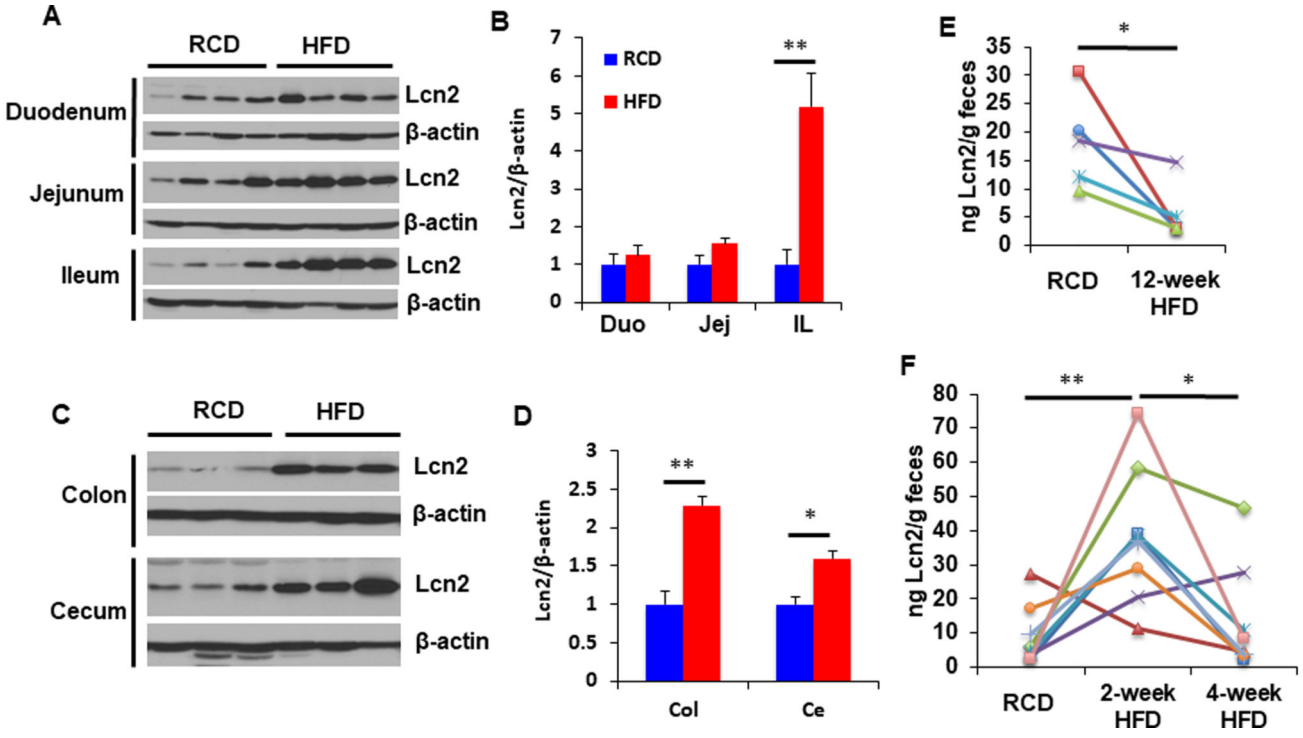

Figure 1: Regulation of Lcn2 expression and secretion in the gut by HFD feeding.

(A-E) Male mice were fed either a RCD or a HFD for 12 weeks and euthanized at the age of 20 weeks. Small intestines (A-B) and large intestines (C-D) were collected and homogenized in RIPA buffer. Lcn2 protein levels were determined by western blotting (A and C) and quantified by ImageJ (B and D). (E-F) Fecal Lcn2 levels were assessed using an ELISA kit. Data are presented as mean ± SEM. (B, D and E). Data was analyzed using a two-tailed unpaired student t-test (B, D, and E) or one-way ANOVA with the Tukey HSD post hoc test (F). n = 4 (B); n = 3 (D); n = 5 (E); n =8 (F). * $P < 0.05$, ** $P < 0.01$.

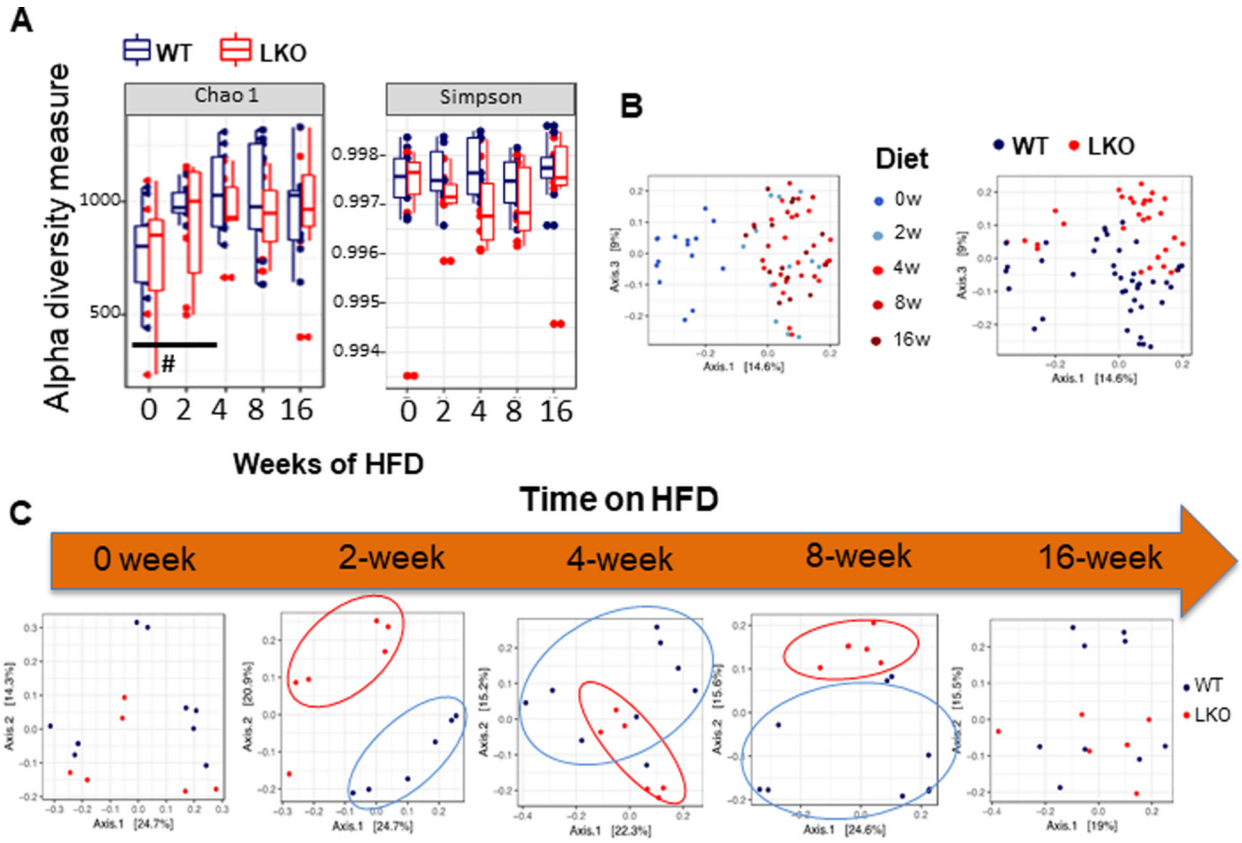

Figure 2: HFD-induced reshaping of gut microbiota in LKO mice.

Male WT mice (n = 9, 3 cages) and LKO mice (n = 7, 3 cages) were fed a HFD starting at the age of 8 weeks. Fecal samples were collected at 0 (RCD), 2, 4, 8 and 16 weeks of HFD feeding. (A) Alpha diversity metrics: Chao1 and Simpson were shown to demonstrate the richness and evenness of gut microbiota communities. (B-C) Beta diversity (unweighted unifrac) indicates the dissimilarity for all-time points (B), the genotypic difference at each time point (C). Data Analysis: (A) Chao1: Repeated measures ANOVA for WT and LKO, followed by the post hoc test Tukey's; Simpson: linear quantile mixed model, followed by a FDR-based multiple testing correction procedure. At all time points, n = 9 for WT; n = 7 for LKO. # $P < 0.05$ versus RCD-fed WT.

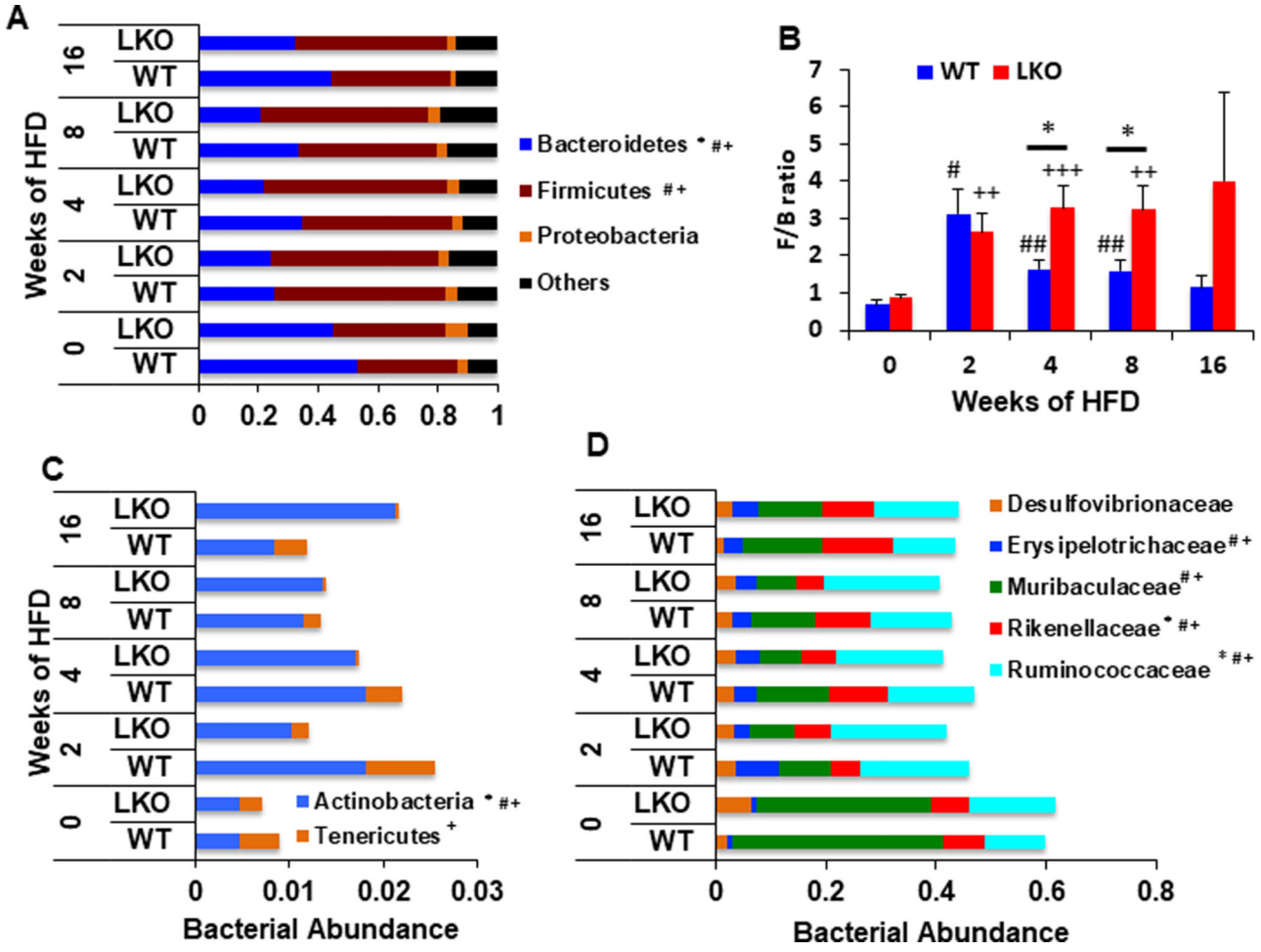

Figure 3: HFD-induced reshaping of gut microbiota in LKO mice.

(A and C) Distribution of bacteria at the phylum level, (B) The ratio of Firmicutes to Bacteroidetes (F/B), and (D) Distribution of bacteria at the major families between WT and LKO mice fed a HFD at all different time points. Data are presented as mean (A, C and D) or as mean ± SEM (B). Data was analyzed using a linear quantile mixed model, followed by a FDR-based multiple testing correction procedure. At all time points, n = 9 for WT; n = 7 for LKO. * $q < 0.05$ versus WT mice at indicated time point. $^{\#}$ $q < 0.05$, $^{\#\#}$ $q < 0.01$ versus RCD-fed WT. $^{+}$ $q < 0.05$, $^{++}$ $q < 0.01$, $^{+++}$ $q < 0.001$, versus RCD-fed LKO mice.

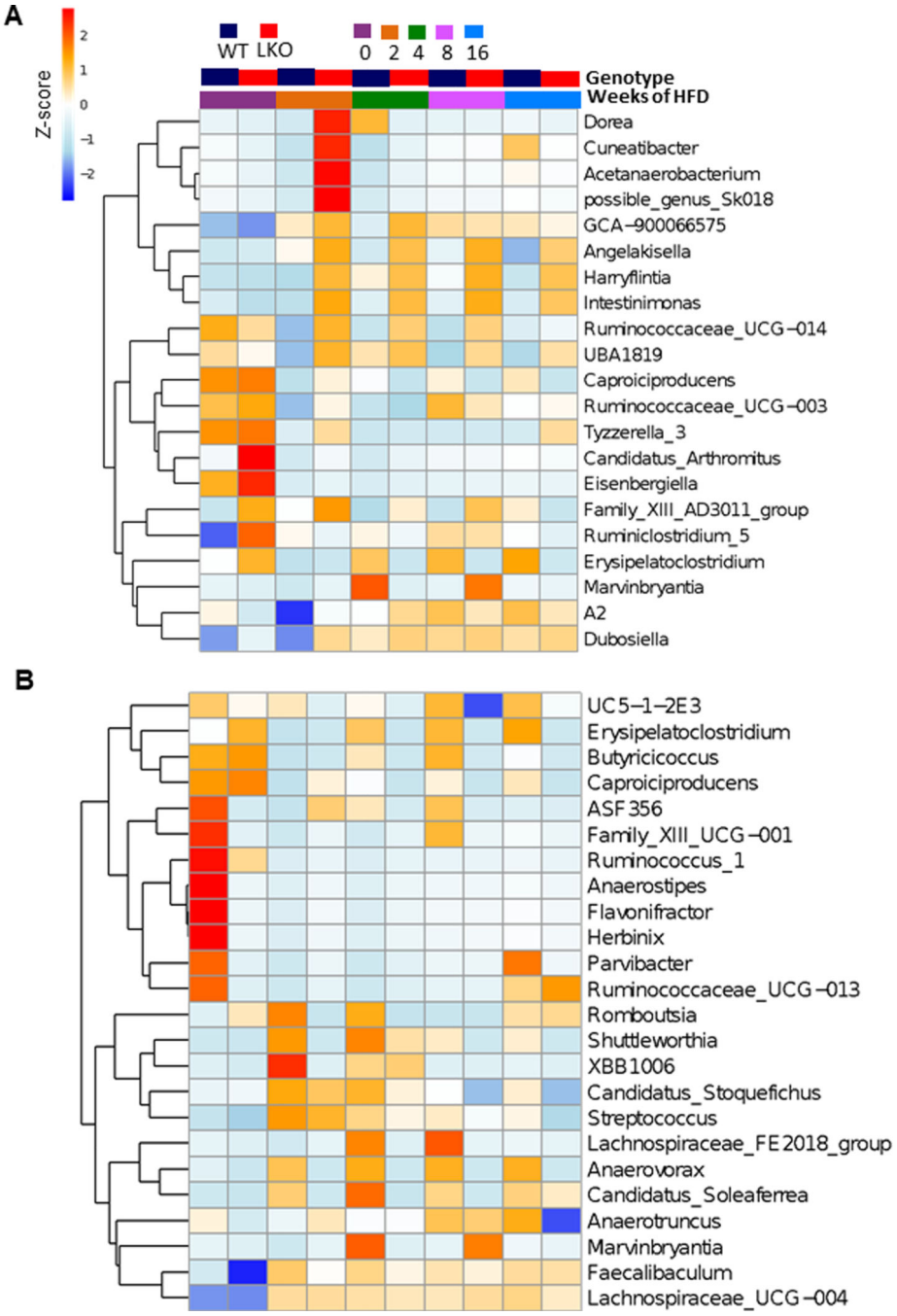

Figure 4: Identification of differentially abundant bacteria between WT and LKO mice.

Shown are hierarchal clustering analysis (HCA)-based heatmaps on differentially abundant microbes at the genus level between WT (n = 9) and LKO (n = 7) mice based on a negative binomial generalized linear model. The bacteria with significantly increased (A) and decreased (B) abundances in LKO mice. q value < 0.05 and log2 scale fold change > 1 are the criteria to determine the significance. n = 9 for WT; n = 7 for LKO.

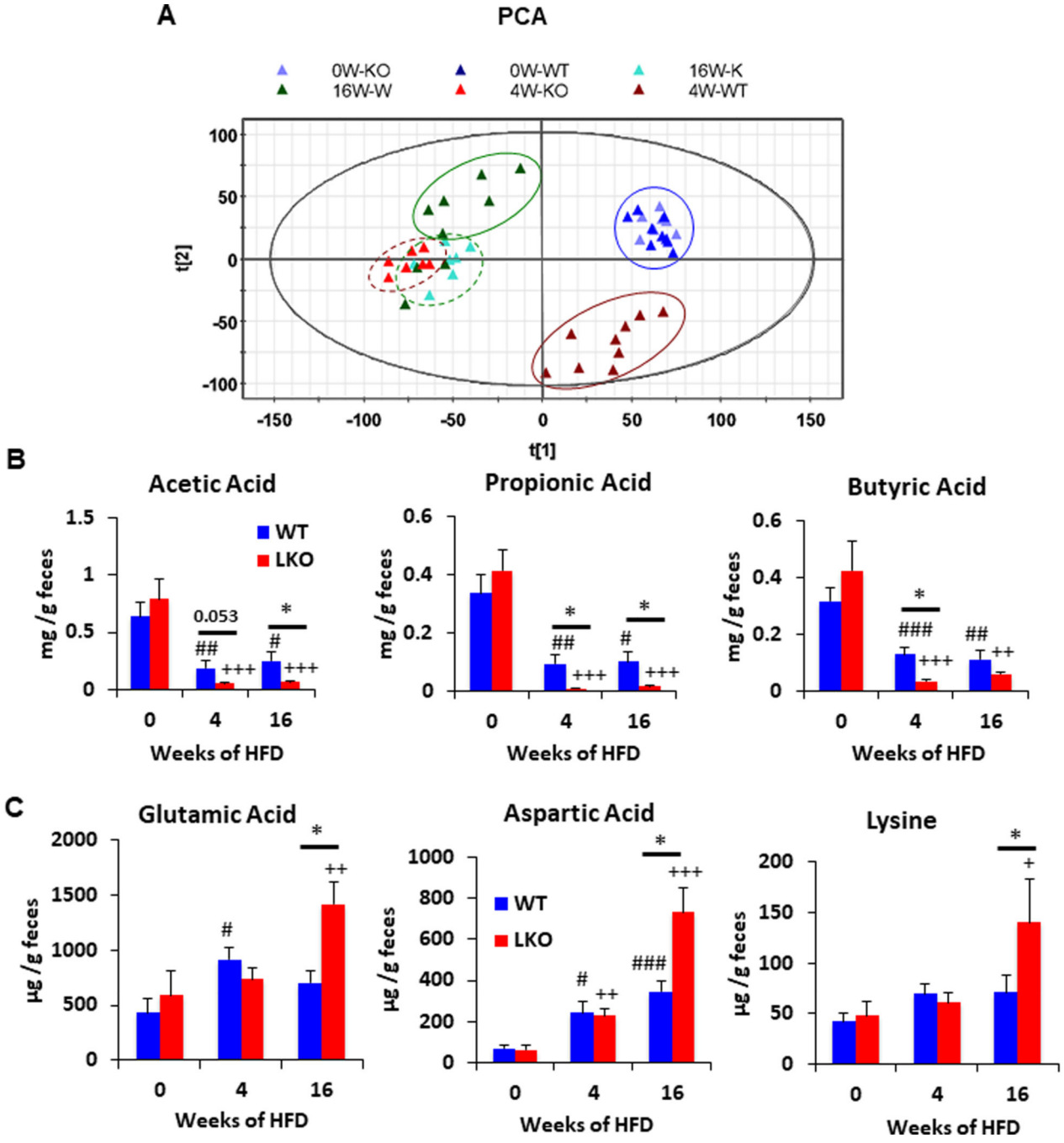

Figure 5: Remodeling of fecal metabolites in LKO mice during HFD consumption.

Stool samples from WT and LKO mice fed a HFD for 0, 4, and 16 weeks were homogenized in 50% ACN. (A) Data from LC-MS analyses of fecal extracts were processed by principal component analysis (PCA) modeling. Shown is the scores plot of a PCA model on the metabolites in fecal extracts. (B-C) Supernatants were collected either for HQ reaction to detect SCFAs (B) or for DC reaction to detect amino acids (C). Data are presented as mean ± SEM and analyzed using a linear quantile mixed model, followed by a FDR-based multiple testing correction procedure. At all time points, n = 9 for WT; n = 7 for LKO. * $q <$

0.05 versus WT mice at indicated time point. $^{\#}$ $q < 0.05$, $^{\#\#}$ $q < 0.01$, $^{\#\#\#}$ $q < 0.001$ versus RCD-fed WT. $^{+}$ $q < 0.05$, $^{++}$ $q < 0.01$, $^{+++}$ $q < 0.001$ versus RCD-fed LKO mice.

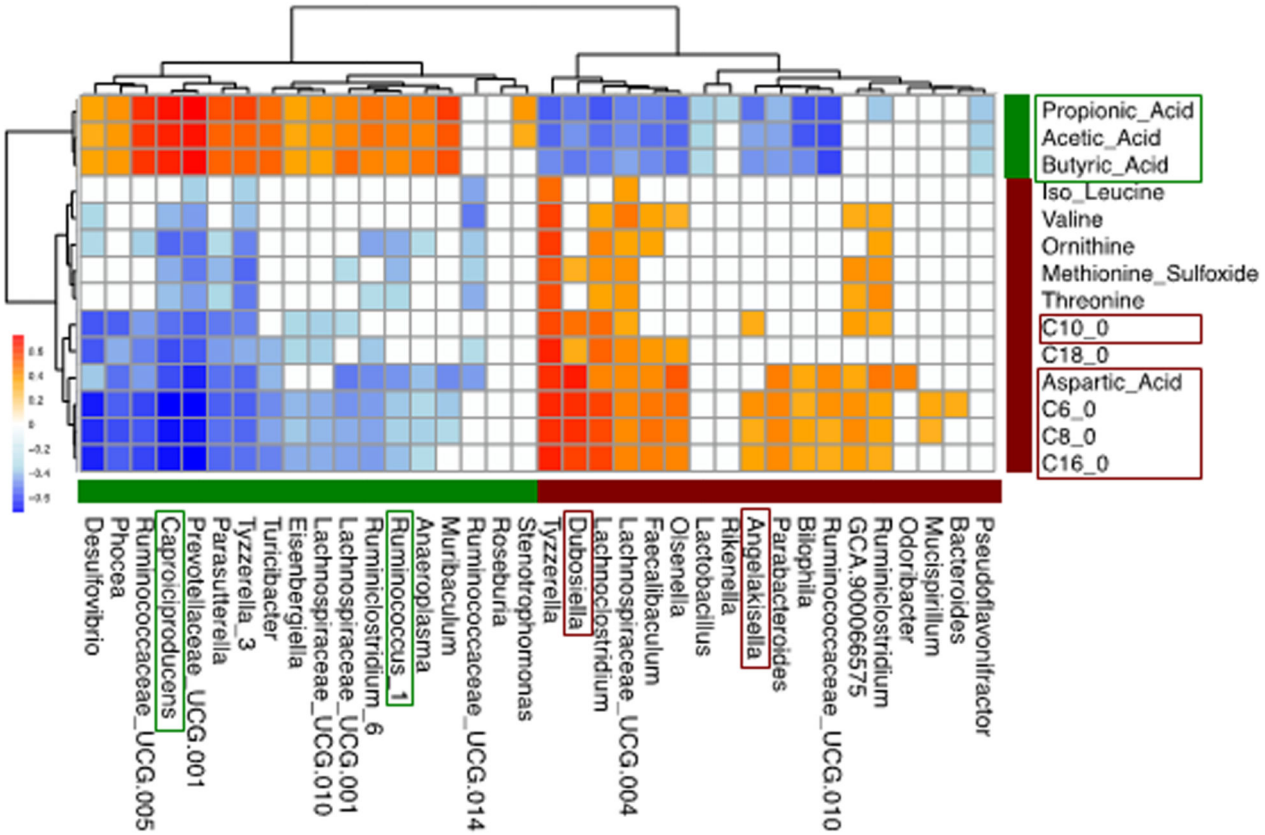

Figure 6: Correlation of body weight with microbes and metabolites.

The correlations between body weight, bacteria and metabolites were evaluated by Spearman's correlation analyses. *P*-values were corrected by the Benjamini-Hochberg method. $P < 0.05$ is considered to be significantly associated. Body weight was significantly associated with 14 fecal metabolites, including 3 short-chain fatty acids (negatively in dark green bar), 5 medium/long-chain fatty acids and 6 amino acids (positively in dark red bar), as well as significantly associated with 36 bacteria at the genus level (18 negatively in dark green bar, 18 positively in dark red bar). HCA-based heatmap showed the correlation between the selected fecal metabolites and microbes. Based on the values of Spearman's rho, Red tiles indicate positive associations and blue tiles negative associations; gray tiles indicate non-significant associations ($P > 0.05$). Bacteria and metabolites labeled by red rectangle were significantly increased in LKO mice, while those labeled by green were decreased in LKO.

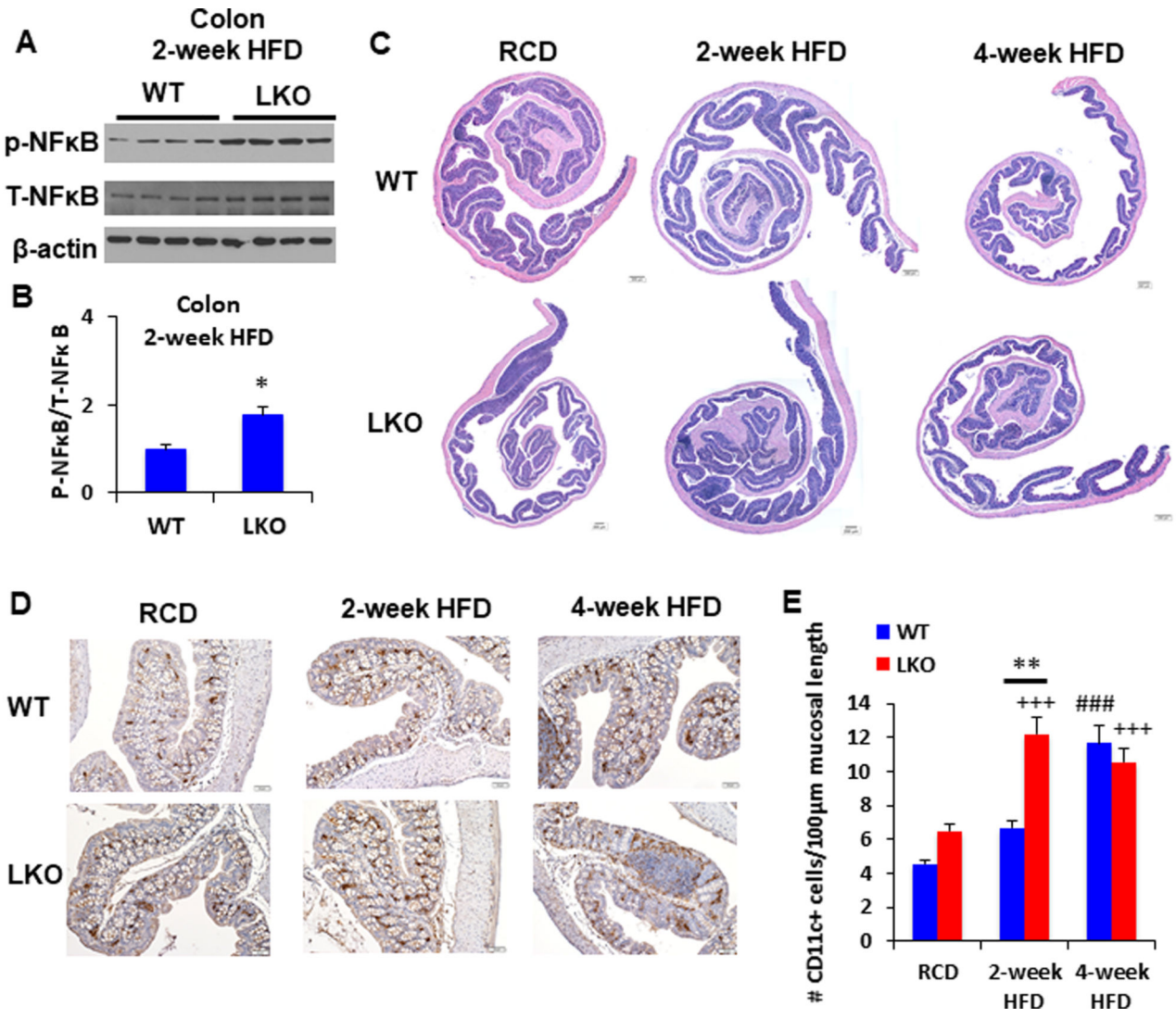

Figure 7: Time-dependent effect of HFD on intestinal inflammation in LKO mice.

(A-B) Colon tissues were collected from male WT and LKO mice fed a HFD for 2 weeks for the examination of phosphor (S536)-NFκB and total NFκB levels by western blotting (A) and quantified by ImageJ (B). (C) H&E staining of colon from RCD-fed or HFD-fed male WT and LKO mice. Scale bars = 200 μm, x 200. (D-E) Immunohistochemistry of CD11c on paraffin-embedded colon sections from RCD-fed, 2-week HFD-fed, 4-week HFD-fed WT and LKO male mice. (D) Representative images of CD11c stained colon sections, scale bars = 50 μm, x200. (E) Results were quantified by counting the number of $CD11c^{+}$ cells and measuring the mucosal length. Data are presented as mean ± SEM. Data was analyzed by a two-tailed unpaired student t-test (B) or 2-way ANOVA with the post hoc test Tukey's; the genotype and diet interaction *P*-value < 0.001 (E). n = 5 for both WT and LKO on RCD and 2-week HFD; n = 6 for both WT and LKO on 4-week HFD; n = 9 for WT and n = 7 for LKO on 16-week HFD. * $P < 0.05$, ** $P < 0.01$ versus WT mice. $^{\#}$ $P < 0.05$,

$P < 0.001$ versus RCD-fed WT. + $P < 0.05$, ++ $P < 0.01$, +++ $P < 0.001$ versus RCD-fed LKO mice.